Article

How Does the cAMP-Dependent Protein Kinase Catalyze the Phosphorylation Reaction: An ab Initio QM/MM Study

Yuhui Cheng, Yingkai Zhang, and J. Andrew McCammon

J. Am. Chem. Soc., **2005**, 127 (5), 1553-1562• DOI: 10.1021/ja0464084 • Publication Date (Web): 15 January 2005

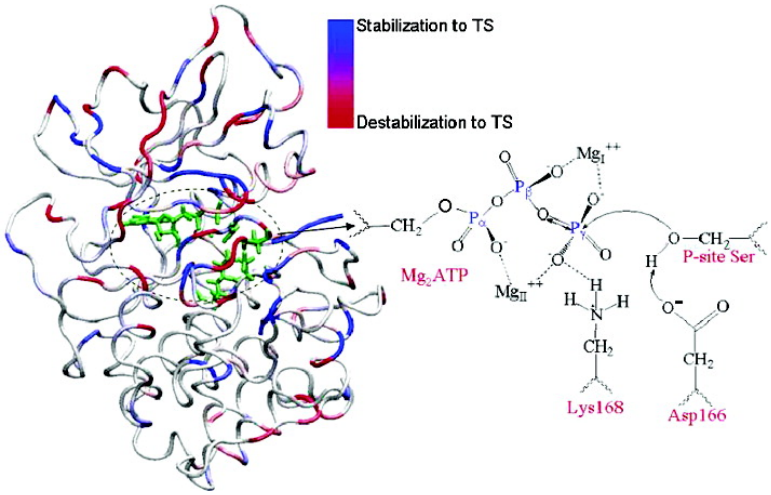

More About This Article

Additional resources and features associated with this article are available within the HTML version:

- Supporting Information
- Links to the 17 articles that cite this article, as of the time of this article download
- Access to high resolution figures
- Links to articles and content related to this article
- Copyright permission to reproduce figures and/or text from this article

View the Full Text HTML

J|A|C|S
ARTICLES
Published on Web 01/15/2005

How Does the cAMP-Dependent Protein Kinase Catalyze the Phosphorylation Reaction: An ab Initio QM/MM Study

Yuhui Cheng,*,† Yingkai Zhang,‡ and J. Andrew McCammon†

Contribution from the Howard Hughes Medical Institute, Department of Chemistry and Biochemistry and Department of Pharmacology, University of California at San Diego, La Jolla, California 92093-0365, and Department of Chemistry, New York University, New York, New York 10003

Received June 17, 2004; E-mail: ycheng@mccammon.ucsd.edu

Abstract: We have carried out density functional theory QM/MM calculations on the catalytic subunit of cAMP-dependent protein kinase (PKA). The QM/MM calculations indicate that the phosphorylation reaction catalyzed by PKA is mainly dissociative, and Asp166 serves as the catalytic base to accept the proton delivered by the substrate peptide. Among the key interactions in the active site, the Mg^{2+} ions, glycine rich loop, and Lys72 are found to stabilize the transition state through electrostatic interactions. On the other hand, Lys168, Asn171, Asp184, and the conserved waters bound to Mg^{2+} ions do not directly contribute to lower the energy barrier of the phosphorylation reaction, and possible roles for these residues are proposed. The QM/MM calculations with different QM/MM partition schemes or different initial structures yield consistent results. In addition, we have carried out 12 ns molecular dynamics simulations on both wild type and K168A mutated PKA, respectively, to demonstrate that the catalytic role of Lys168 is to keep ATP and substrate peptide in the near-attack reactive conformation.

1. Introduction

Protein phosphorylation, a common reversible covalent modification catalyzed by protein kinases, plays a critical role in cellular regulation and signal transduction. There are more than 500 protein kinase genes identified, representing about 1.7% of all human genes. In the large and very diverse family of protein kinases, the catalytic subunit (C-subunit) of cyclic AMP-dependent protein kinase (PKA) is the best characterized member and often serves as a paradigm for the entire family.[1] This subunit has only about 350 residues and a bilobal structure. It catalyzes the transfer of γ-phosphate of ATP to specific serine or threonine residues of the substrate peptides. Experimentally, it was the first protein kinase to be discovered and purified,[2] the first to be sequenced,[3] and the first to be cloned and expressed in large quantities in *Escherichia coli*.[4]

Extensive experimental studies have been reported, including mutagenesis,[5−11] NMR solution studies, chemical footprints, catalytic trapping, rapid quench flow, mass spectrometry, fluorescence anisotropy,[1,9,12−15] and crystal structures of several complexes (including reactant and transition state mimics).[16−19] Much information has been provided. However, due to experimental challenges in defining the reaction mechanism, some detailed questions regarding how PKA catalyzes the phosphorylation reaction remain unsettled, including whether the reaction is associative or dissociative and the respective catalytic roles of specific residues, metal ions, and structural elements. There are particularly intriguing questions regarding the catalytic roles of Asp166, Lys168, the glycine rich loop, etc.

Asp166 is a residue conserved in the active site of all protein kinases and resides in a position likely to form hydrogen bonds with the substrate Ser.[19,20] Mutation to Ala causes at least a 300-fold reduction of the V_{max} without greatly affecting the K_m's for either ATP or the substrate peptide.[5] It was first suggested to be the catalytic base, which accepts the proton from the

† University of California at San Diego.
‡ New York University.

(1) Johnson, D. A.; Akamine, P.; Radzio-Andzelm, E.; Madhusudan; Taylor, S. S. *Chem. Rev.* **2001**, *101*, 2243−2270.
(2) Walsh, D. A.; Perkins, J. P.; Krebs, E. G. *J. Biol. Chem.* **1968**, *243*, 3763−3774.
(3) Shoji, S.; Titani, K.; Demaille, J. G.; Fischer, E. H. *J. Biol. Chem.* **1979**, *254*, 6211−6214.
(4) Slice, L. W.; Taylor, S. S. *J. Biol. Chem.* **1989**, *264*, 20940−20946.
(5) Gibbs, C. S.; Zoller, M. J. *J. Biol. Chem.* **1991**, *266*, 8923−8931.
(6) Gibbs, C. S.; Knighton, D. R.; Sowadski, J. M.; Taylor, S. S.; Zoller, M. J. *J. Biol. Chem.* **1992**, *267*, 4806−4814.
(7) Adams, J. A.; McGlone, M. L.; Gibson, R.; Taylor, S. S. *Biochemistry* **1995**, *34*, 2447−2454.
(8) Yonemoto, W.; McGlone, M. L.; Grant, B.; Taylor, S. S. *Protein Eng.* **1997**, *10*, 915−925.
(9) Grant, B. D.; Adams, J. A. *Biochemistry* **1996**, *35*, 2022−2029.
(10) Hemmer, W.; McGlone, M.; Tsigelny, I.; Taylor, S. S. *J. Biol. Chem.* **1997**, *272*, 16946−16954.
(11) Aimes, R. T.; Hemmer, W.; Taylor, S. S. *Biochemistry* **2000**, *39*, 8325−8332.
(12) Seifert, M. H. J.; Breitenlechner, C. B.; Bossemeyer, D.; Huber, R.; Holak, T. A.; Engh, R. A. *Biochemistry* **2002**, *41*, 5968−5977.
(13) Lew, J.; Coruh, N.; Tsigelny, I.; Garrod, S.; Taylor, S. S. *J. Biol. Chem.* **1997**, *272*, 1507−1513.
(14) Shaffer, J.; Adams, J. A. *Biochemistry* **1999**, *38*, 12072−12079.
(15) Cheng, X. D.; Shaltiel, S.; Taylor, S. S. *Biochemistry* **1998**, *37*, 14005−14013.
(16) Madhusudan; Akamine, P.; Xuong, N. H.; Taylor, S. S. *Nat. Struct. Biol.* **2002**, *9*, 273−277.
(17) Bossemeyer, D.; Engh, R. A.; Kinzel, V.; Ponstingl, H.; Huber, R. *EMBO J.* **1993**, *12*, 849−859.
(18) Yang, J.; Ten eyck, L. F.; Xuong, N. H.; Taylor, S. S. *J. Mol. Biol.* **2004**, *336*, 473−487.
(19) Madhusudan; Trafny, E. A.; Xuong, N. H.; Adams, J. A.; Teneyck, L. F.; Taylor,S. S.; Sowadski, J. M. *Protein Sci.* **1994**, *3*, 176−187.
(20) Zheng, J. H.; Knighton, D. R.; Xuong, N. H.; Taylor, S. S.; Sowadski, J. M.; Teneyck, L. F. *Protein Sci.* **1993**, *2*, 1559−1573.

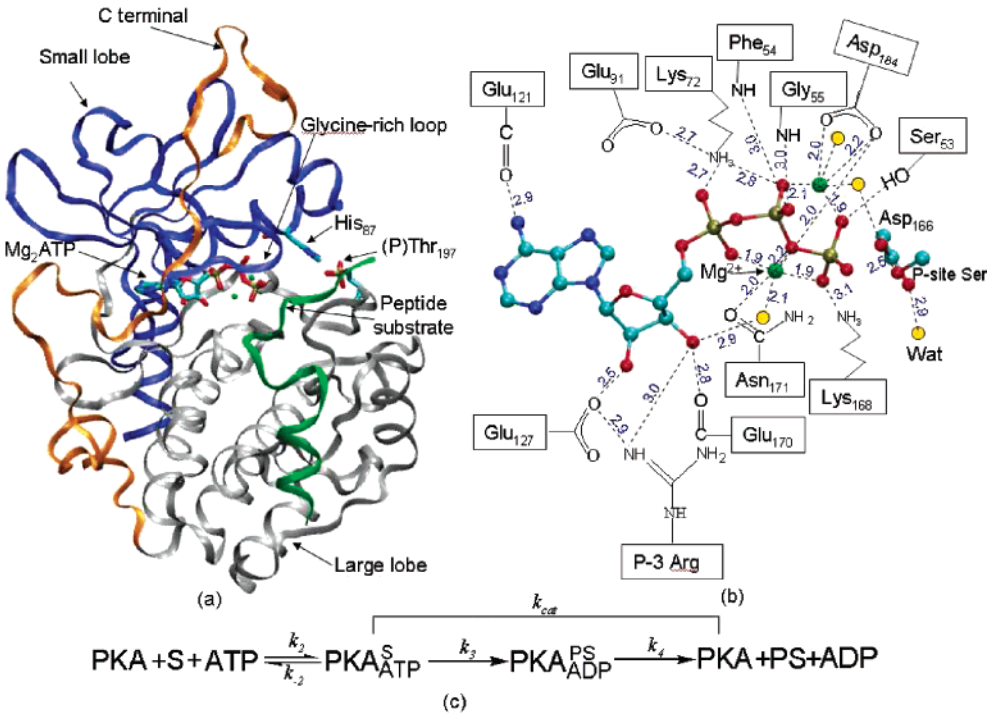

Figure 1. The structure of the ternary PKA−substrate complex. (a) Ribbon representation of the catalytic subunit with the N-terminal (in purple), small-lobe core (in blue), large-lobe core (in tan), and the C-terminal (in orange), including Mg_2ATP (in licorice representation) and a 20-residue peptide substrate (in green) resulting from the initial MM geometry optimization. (b) The schematic representation of the active site. Residues displayed in ball-and-stick representation exhibit the exact conformation and relative orientation, including ATP ligand side chains of P-site Ser and Asp166, two Mg ions (in green), and three conserved waters (in yellow). (c) The overall phosphoryl-transfer reaction scheme. k_3 is the rate constant of the phosphoryl-transfer step, and k_4 is the rate constant of the product-release step. k_{cat} is the first-order rate constant for the overall phosphoryl transfer and product release.

substrate hydroxyl and enhances the nucleophilic reactivity of the P-site serine. This suggestion is consistent with the early pH dependence studies,[21] which indicate that there is a catalytic base existing in the active site. However, more recent kinetic studies in which the burst phase in PKA activity was monitored with rapid quench flow techniques have shown that the rate constant for this phase is independent of pH between pH 6 and 9.[22] Meantime, considering the basicities of aspartate (pK_a of less than 5) and serine (pK_a of 14) in the aqueous solvent, it was suggested that Asp166 may not be an effective general base, and the catalytic roles for Asp166 may be the substrate orientation or to accept the proton late in the reaction process.[22] Lys168 is another important residue in the PKA active site. It is conserved in all Ser/Thr kinases and replaced by an Arg in tyrosine kinases.[23,24] It interacts with γ-phosphate in various crystal structures before and after phosphoryl transfer,[19] and the replacement of Lys168 with Ala leads to a 50-fold reduction of the k_{cat}. Although Lys168 is recognized to be important, the respective catalytic role is not clear: whether stabilizing the transition state through electrostatic interaction, or directly participating in the reaction by transferring one of its protons to the phosphate group, or something else. The glycine-rich loop [KTLG^{50}TG^{52}SFG^{55}RV] in the small lobe is one of the most important motifs in the conserved protein kinase catalytic core. With ATP in the active site cleft, the glycine-rich loop takes on a "U" shape and covers ATP with stable hydrophobic interactions and hydrogen bonding (cf. Figure 1). The analysis of different PKA crystal structures shows that the conformation of this loop is quite related to the ATP loading and the release of ADP product.[25] Structural studies[16] suggest that the loop may play a role in stabilizing the transition state. However, Ala/Ser mutagenesis studies demonstrated that mutations to single glycines had little effect on the catalytic activity of PKA. The most severe effect on k_{cat} was no larger than 6-fold.[10] Other studies showed that the replacement of Ser53 with Thr, Gly, or Pro did not affect k_{cat}.[11] It seems that there are some inconsistencies between the suggestions from the structural studies and the results from the mutation studies.

Considering the significance of the phosphorylation reaction and the uncertainties of the experimental studies, computational study of the phosphoryl transfer reaction catalyzed by PKA should be helpful. In principle, computational studies can provide detailed information and insights to complement experimental studies. However, this goal can only be attained when appropriate computational approaches are employed and the system studied is a good mimic of the enzyme system. Early semiempirical QM (AM1, PM3) or semiempirical QM/MM calculations on the phosphorylation reaction catalyzed by kinase[26−28] suggested very high energy barriers and a minimal role of Asp166. Their calculations suggest that the proton in

(21) Yoon, M. Y.; Cook, P. F. *Biochemistry* **1987**, *26*, 4118−4125.
(22) Zhou, J.; Adams, J. A. *Biochemistry* **1997**, *36*, 2977−2984.
(23) Hanks, S. K.; Quinn, A. M. *Methods Enzymol.* **1991**, *200*, 38−62.
(24) Knighton, D. R.; Cadena, D. L.; Zheng, J. H.; Teneyck, L. F.; Taylor, S. S.; Sowadski, J. M.; Gill, G. N. Structural features that specify tyrosine kinase-activity deduced from homology modeling of the epidermal growth-factor receptor. *Proc. Natl. Acad. Sci. U.S.A.* **1993**, *90* (11).
(25) Li, F.; Gangal, M.; Juliano, C.; Gorfain, E.; Taylor, S. S.; Johnson, D. A. *J. Mol. Biol.* **2002**, *315*, 459−469.
(26) Hart, J. C.; Sheppard, D. W.; Hillier, I. H.; Burton, N. A. *Chem. Commun.* **1999**, 79−80.
(27) Hart, J. C.; Hillier, I. H.; Burton, N. A.; Sheppard, D. W. *J. Am. Chem. Soc.* **1998**, *120*, 13535−13536.
(28) Hutter, M. C.; Helms, V. *Protein Sci.* **1999**, *8*, 2728−2733.

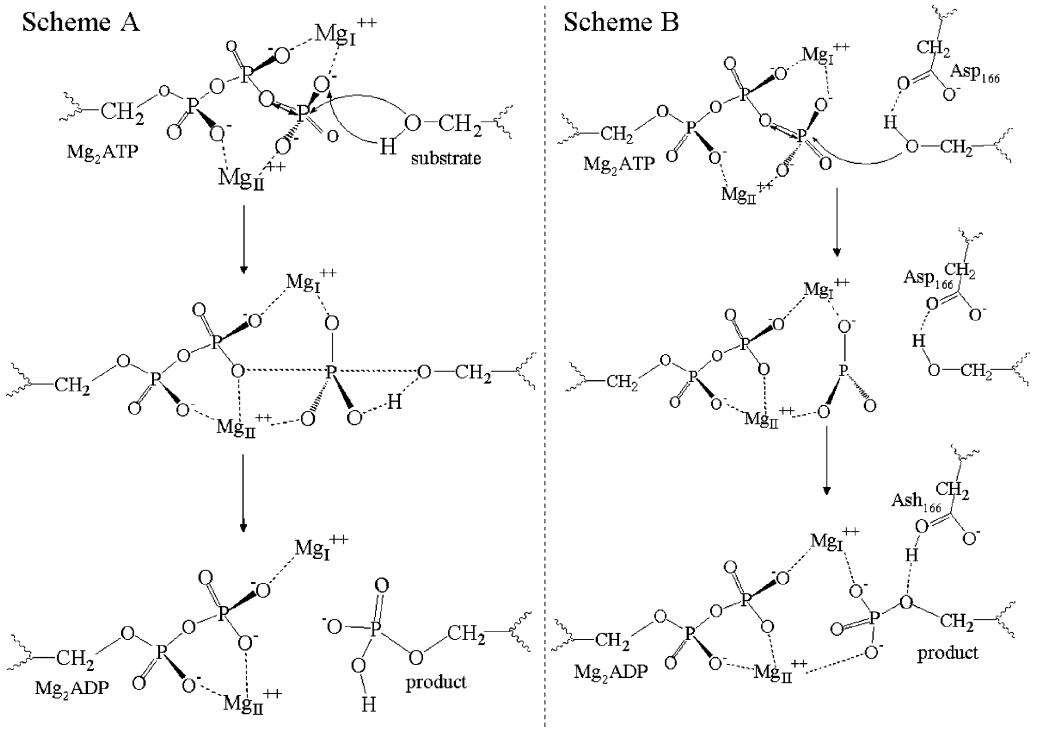

Figure 2. Two phosphoryl transfer schemes provided by previous theoretical calculations. Scheme A is the concerted phosphoryl and proton-transfer model suggested by previous semiempirical calculations and some DFT calculations;[26−28,30,32] scheme B described a dissociative phosphoryl transfer and the shift of the proton to Asp166, which was suggested by the most recent DFT calculations.[33−35]

the substrate hydroxyl directly transfers to γ-phosphate of ATP with or even without the aid of Asp166. The results are inconsistent with the experimental results. Furthermore, ab initio QM calculations and hybrid B3LYP/MM single point calculations by Sheppard et al.[29] have shown that semiempirical methods may not be adequate to study the phosphorylation reaction catalyzed by kinases. Recently, several density functional calculations[30−35] on kinase model complexes have been carried out to study the phosphorylation reaction. In such model complex studies, the size of the system is limited, the enzyme environment cannot be simulated, and the calculation results are often quite dependent on the choice of model complexes. For example, the calculation results by Hirano et al.[30] and Cavalli et al.[32] yielded the reaction scheme A as shown in Figure 2 and obtained a high reaction barrier of 36−42 kcal/mol, while Valiev et al.[33] and Diaz et al.[34] obtained a dissociative reaction pathway (scheme B in Figure 2) with reaction barriers between 10 and 20 kcal/mol. Very recently, Henkelman et al. provided further evidences that the reaction barrier is quite dependent on the model size and initial crystal structures.[35]

In this work, we have performed computational studies on the phosphoryl transfer catalyzed by PKA using combined ab initio quantum mechanical and molecular mechanical (QM/MM) methods. In the study, the whole enzyme complex is simulated. The active site, which participates in making and breaking bonds, is treated by ab initio quantum mechanical methods, while the rest of the enzyme is described by molecular mechanical methods. Calculations with different QM/MM partition schemes and different initial structures yield consistent results, which indicate that the phosphorylation reaction catalyzed by PKA is mainly dissociative and that Asp166 serves as the catalytic base to accept the proton delivered by the substrate peptide. Furthermore, we have elucidated the respective catalytic roles of the key interactions throughout the PKA enzyme through reaction barrier decomposition analysis and long molecular dynamics simulations on wild type as well as mutated PKA complexes. The catalytic role of Lys168 is demonstrated to keep ATP and substrate peptide in the near-attack reactive conformation.[36]

2. Computational Methods

In the current study, we employed the pseudobond ab initio QM/MM approach,[37−39] which has been demonstrated to be effective in the study of several enzymes, including enolase,[40] acetylcholinesterase,[41,42] and 4-oxalocrotonate tautomerase.[43,44] Throughout the study,

(29) Sheppard, D. W.; Burton, N. A.; Hillier, I. H. *THEOCHEM* **2000**, *506*, 35−44.
(30) Hirano, Y.; Hata, M.; Hoshino, T.; Tsuda, M. *J. Phys. Chem. B* **2002**, *106*, 5788−5792.
(31) Ginalski, K.; Grochowski, P.; Lesyng, B.; Shugar, D. *Int. J. Quantum Chem.* **2002**, *90*, 1129−1139.
(32) Cavalli, A.; De vivo, M.; Recanatini, M. *Chem. Commun.* **2003**, 1308−1309.
(33) Valiev, M.; Kawai, R.; Adams, J. A.; Weare, J. H. *J. Am. Chem. Soc.* **2003**, *125*, 9926−9927.
(34) Diaz, N.; Field, M. J. *J. Am. Chem. Soc.* **2004**, *126*, 529−542.
(35) Henkelman, G.; LaBute, M. X.; Tung, C. S.; Fenimore, P. W.; McMahon, B. H. To be published.
(36) Hur, S.; Bruice, T. C. The near attack conformation approach to the study of thechorismate to prephenate reaction. *Proc. Natl. Acad. Sci. U.S.A.* **2003**, *100* (21).
(37) Zhang, Y. K.; Lee, T. S.; Yang, W. T. *J. Chem. Phys.* **1999**, *110*, 46−54.
(38) Zhang, Y. K.; Liu, H. Y.; Yang, W. T. *J. Chem. Phys.* **2000**, *112*, 3483−3492.
(39) Zhang, Y.; Liu, H.; Yang, W. Ab Initio QM/MM and Free Energy Calculations of Enzyme Reactions. In *Methods for Macromolecular Modeling*; Schlick, T., et al., Eds.; Springer-Verlag: 2001.
(40) Liu, H. Y.; Zhang, Y. K.; Yang, W. T. *J. Am. Chem. Soc.* **2000**, *122*, 6560−6570.
(41) Zhang, Y. K.; Kua, J.; McCammon, J. A. *J. Am. Chem. Soc.* **2002**, *124*, 10572−10577.
(42) Zhang, Y. K.; Kua, J.; McCammon, J. A. *J. Phys. Chem. B* **2003**, *107*, 4459−4463.

the charged phosphate groups were included in the QM subsystem and were calculated at the B3LYP/6-31G* level. This level of calculation is similar to that used in other contemporary studies.[33,34]

2.1. Preparation of the Enzyme−Substrate System. The initial structure was chosen from two PKA−ligand complexes (PDB code: 1L3R and 1ATP). The 1L3R structure is that of PKA in complex with ADP, AlF_3, and Mg^{2+}, while the 1ATP structure is that of a ground state analogue in which the thermally stable inhibitor PKI instead of the substrate peptide (SP20) is included. For the 1L3R structure, we mutated AlF_3 back to γ-phosphate using Insight II. For the 1ATP structure, we phosphorylated Ser139, replaced two Mn^{2+} with Mg^{2+} ions, and mutated the P-1 and P site residues of PKI to change it into the substrate peptide (SP20). For both 1L3R and 1ATP models, hydrogens for heavy atoms were added by Leap in the Amber 7.0 package,[45] while hydrogens for crystal conserved waters were added and optimized by WHATIF.[46] For histidine residues, calculations of the local electrostatic microenvironment and the effective pK_a with WHATIF indicated that His87 should doubly be protonated on both N_η and N_δ, while the others are neutral residues: HID62, HID68, and HID260 with N_δ protonated; HIE131, HIE142, HIE158, and HIE294 with N_η protonated. Whether HID/HIE is chosen is determined by the local hydrogen bonding network. Since the charge parameters of Mg_2ATP, phosphorylated serine and threonine are not available in the Amber force field, we have determined them using QM calculation and the RESP module in the Amber 7.0 package. All other force field parameters are from the parm99 parameter set[47] and the polyphosphate parameters developed by Meagher et al.[48]

After relaxing the added atoms using the Amber 7.0 package in the gas phase, each structure was immersed in a cubic TIP3P water box ($90 \times 90 \times 90$ Å^3) and neutralized by addition of Cl^- counterions using the Amber Leap module. This led to a 1L3R simulation system of 40 332 atoms and a 1ATP simulation system of 37 117 atoms, respectively. Molecular dynamics simulation with periodic boundary conditions was conducted. A default cutoff radius of 8 Å was introduced for nonbonding interactions, updating the neighbor pair list every 10 steps. The electrostatic interactions were calculated with the Particle Mesh Ewald method.[49] The SHAKE algorithm[50] was used to constrain all bond lengths involving hydrogens. Optimization and 50 ps relaxation of solvent and ions were performed at first under constant volume conditions, keeping all the heavy atoms constrained to their initial positions with a force constant of 50 kcal/mol Å^2, and then under constant pressure and the same constraint, the whole complex was relaxed for 60 ps. The systems were then energy refined with 50 and 20 kcal/mol Å^2 constraints, respectively. The QM/MM model was obtained by deleting the water more than 27.0 Å away from the β-phosphorus of ATP. The total atom numbers in our QM/MM models are 8610 in 1L3R and 9652 in 1ATP. At the same time, free MD simulations of both 1L3R and 1ATP were continued to obtain 12 ns trajectories.

2.2. QM/MM Calculations. The enzyme−substrate models 1L3R and 1ATP prepared as described above were each partitioned into a QM subsystem and a MM subsystem. We have employed two partition schemes, with the sole difference in whether to cut the ATP molecule. In the small QM subsystem partition scheme, the QM subsystem

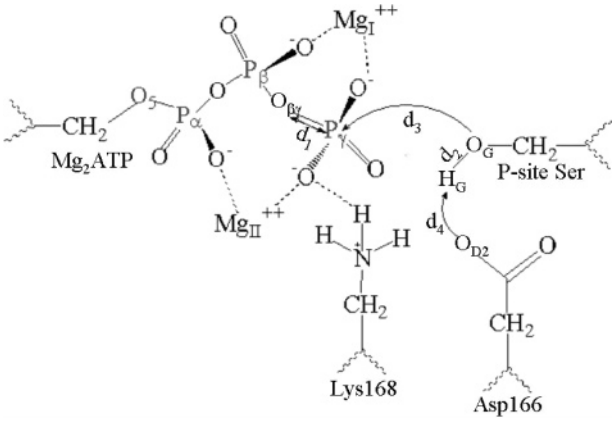

Figure 3. 49-atom QM subgroup in our QM/MM calculations (the small QM/MM model).

comprises the triphosphate arm of ATP, side chains of P-site Ser, Asp166, and Lys168, and two Mg^{2+} ions with 49 atoms. The large QM subsystem consists of the whole ATP molecule, side chains of P-site Ser, Asp166, Lys168, and two Mg^{2+} ions for a total of 75 atoms. The boundary between the QM and MM subsystems was treated using the pseudobond approach.[37] The total energy of the QM/MM system is

$$E_{\text{Total}} = E_{\text{MM}} + E_{\text{QM}} + E_{\text{QM/MM}} \quad (1)$$

The QM/MM interactions consist of bonding and nonbonding interactions. The nonbonding interactions between two subsystems include the vdW part through the Lennard−Jones potential and the electrostatic part calculated through a Coulombic term in an effective Hamiltonian. The energy of the effective Hamiltonian, which is obtained by QM calculations, is the sum of the QM energy of the QM subsystem (E_{QM}) and the electrostatic interaction between QM and MM subsystems.[37]

With each prepared QM/MM system an iterative optimization procedure[38] was applied to the system with B3LYP(6-31G*) QM/MM calculations, leading to an optimized structure for the reactant. We then employed the reaction coordinate driving method[38,51] to search for the transition state and product. By experimenting with several possible reaction coordinates, the following reaction coordinate turns out to be most appropriate for this phosphorylation reaction: $\text{RC} = d_1 + d_3 - d_2 - d_4$, where the definitions of d_1, d_2, d_3, and d_4 are described in Figure 3. An iterative restrained minimization was then repeatedly applied to different points along the reaction coordinate, resulting in a minimum energy path for the reaction in the enzymatic environment and its associated potential energy surface. Given that the determined minimum energy path is smooth and continuous, Hessian matrices for degrees of freedom involving atoms in the QM subsystem were calculated at stationary points, leading to determination of the corresponding vibrational frequencies.[39] The energy maximum on the path with one and only one imaginary frequency is the transition state, while the energy minima along the path with no imaginary frequencies are characterized as the reactant or the intermediate. For the reactant, transition state, and tetrahedral intermediate, we further carried out single-point higher level (MP2 and B3LYP) QM/MM calculations with a larger 6-31+G* basis set.

2.3. Other Computational Details. Geometry optimizations for all the above QM subgroups were at the B3LYP(6-31G*) level, with the interactions from the MM subgroup treated by the QM/MM method. The subsequent single-point calculations at the 6-31+G* level with B3LYP and MP2 were performed on the geometries optimized at the B3LYP(6-31G*) level. Throughout the QM/MM calculations, pseudo-

(43) Cisneros, G. A.; Liu, H. Y.; Zhang, Y. K.; Yang, W. T. *J. Am. Chem. Soc.* **2003**, *125*, 10384−10393.
(44) Cisneros, G. A.; Wang, M.; Silinski, P.; Fitzgerald, M. C.; Yang, W. T. *Biochemistry* **2004**, *43*, 6885−6892.
(45) Case, D. A. et al. *Amber 7.0*; University of California: San Francisco, CA, 2002.
(46) Vriend, G. *J. Mol. Graphics* **1990**, *8*, 52−56.
(47) Cornell, W. D.; Cieplak, P.; Bayly, C. I.; Gould, I. R.; Merz, K. M.; Ferguson, D. M.; Spellmeyer, D. C.; Fox, T.; Caldwell, J. W.; Kollman, P. A. *J. Am. Chem. Soc.* **1995**, *117*, 5179−5197.
(48) Meagher, K. L.; Redman, L. T.; Carlson, H. A. *J. Comput. Chem.* **2003**, *24*, 1016−1025.
(49) Darden, T.; York, D.; Pedersen, L. *J. Chem. Phys.* **1993**, *98*, 10089−10092.
(50) Ryckaert, J. P.; Ciccotti, G.; Berendsen, H. J. C. *J. Comput. Phys.* **1977**, *23*, 327−341.
(51) Williams, I. H.; Maggiora, G. M. *THEOCHEM* **1982**, *6*, 365−378.

Table 1. Calculated Total QM/MM Potential Energy Difference (kcal/mol) for Three QM/MM Models (the Geometries Are Calculated at the B3LYP(6-31G*)/MM Level)

	MP2(6-31+G*)/MM	B3LYP(6-31+G*)/MM	B3LYP(6-31G*)/MM
	1L3R Small Model		
reactant	0.0	0.0	0.0
transition state	9.1	11.6	10.9
intermediate	6.6	9.5	7.8
	1ATP Small Model		
reactant	0.0	0.0	0.0
transition state	11.6	14.3	12.3
intermediate	10.1	12.6	10.4
	1L3R Large Model		
reactant	0.0	0.0	0.0
transition state	7.7	10.0	9.5
intermediate	4.3	7.4	6.3

bonds were treated with the 3-21G basis set and its corresponding effective core potential parameters. The calculations were carried out using modified versions of the Gaussian98 and TINKER programs.[52] For the QM subsystem, criteria used for geometry optimizations follow Gaussian98 defaults. For the MM subsystem, the convergence criterion used is to have the root-mean-square (RMS) energy gradient be less than 0.1 kcal mol^{-1} $Å^{-1}$. In the MM minimizations, only atoms within 20 Å of the β phosphorus of ATP were allowed to move. No cutoff for nonbonding interactions was used in the QM/MM calculations and the MM minimizations.

3. Results and Discussions

For the phosphoryl-transfer reaction step, the calculated potential energy results are listed in Table 1, and the reaction energy profiles and the corresponding geometries for the reactant, transition state, and the intermediate are shown in Figure 4. The calculated minimum-energy paths are shown in the Figure 5. Despite the choices of the different initial structures (1L3R vs 1ATP) and the different QM/MM partition schemes, the calculations provide a consistent picture. Our results do not support the mechanism proposed from previous semiempirical QM studies.[26−28] We found that the phosphorylation reaction proceeds through a mainly dissociative transition state, and Asp166 serves as the catalytic base to accept the late proton transfer, which is consistent with the reaction scheme B[33,34] as shown in Figure 2. The calculated potential energy barriers at the B3LYP(6-31+G*) QM/MM level are 11.6, 14.3, and 10.0 kcal/mol for 1L3R (small QM subsystem), 1ATP (small QM subsystem), and 1L3R (large QM subsystem), respectively. The value of the barriers is quite consistent with the experimental measurement of about 500 s^{-1} for the phosphoryl-transfer step (i.e., k_3, cf. Figure 1c).[9] According to the enzymatic reaction rate theory, the relation between the phenomenological reaction barrier and the rate constant can be written as

$$k(T) = (k_B T/h)(c^0)^{1-n} \exp[-\Delta G^\circ_{act}(T)/RT]$$

For our case, the approximate reaction barrier is around 13.8 kcal mol^{-1}.

To test whether reaction scheme A is possible, in which the proton of the P-site serine transfers to the oxygen of the phosphate, we also conducted the corresponding B3LYP(6-31G*) QM/MM calculation using the 1L3R small model and found that the energy barrier is over 20 kcal/mol for reaction scheme A in comparison with 11.6 kcal/mol for the reaction scheme B. So our calculations do not support reaction scheme A in Figure 2.[26−28,30,32] Our reaction barriers are quite close to the recent DFT calculations on the active site of PKA. For example, Valiev et al. proposed an 11.0 kcal/mol reaction barrier, while a barrier of 16.5 kcal/mol was proposed by Diaz et al.[33,34]

From the calculated geometry for the transition state, we can see that the phosphoryl transfer in PKA is mainly dissociative. Both of the QM/MM calculations for 1L3R showed symmetric transition states and ~80% dissociative character using Pauling's formula as suggested by Mildvan.[53] The PO_3 plane is almost in the middle of the entering and leaving oxygens, and the distances between the phosphorus and the entering and leaving oxygens are 2.1 Å and 2.3 Å, respectively. For the 1ATP small QM model, a similar trigonal bipyramidal coordination for the transition state was obtained. PO_3 is in a planar geometry, too. The distances between the phosphorus and the donor and recipient oxygens are 2.5 and 2.0 Å, respectively. Overall, the active site geometries of our transition states are quite similar to the above two DFT calculations.[33,34]

Role of Asp166. Asp166 was confirmed to be the catalytic base again in our calculations. Despite the choice of the different initial crystal structures and different partitions, the calculated distances show that the substrate Ser still keeps its hydroxyl proton at the transition state, which confirms the late proton-transfer result by Valiev et al.[33] and is also consistent with recent experimental results.[16,54−60]

To test the hypothesis that Asp166 also acts as a structural anchor to maintain the configuration of the active site, we have mutated Asp166 to Ala at the beginning of setting up the wild type 1L3R model and then performed 12 ns classical MD simulation using the Amber99 force field for this mutated PKA with the same procedure for the wild type 1L3R. By analyzing the MD trajectories, we did not find a significant change in the configuration of the active site between two simulations; cf. Figure 6. The average distance between γ-phosphorus and the hydroxyl oxygen of substrate Ser is 3.36 ± 0.21 Å for the mutated PKA and 3.72 ± 0.42 Å in the wild type 1L3R model. The mean-square fluctuations of the positions of the ATP atoms are also similar in the two simulations. Such an observation is quite consistent with only a small, 3-fold increase in K_m(pep) and similar K_m(ATP) in D166A mutation experiments.[5] So our QM/MM and MD simulation results indicate that the role of Asp166 is as the catalytic base, rather than a structural anchor to maintain the configuration.

Role of Lys168. Besides Asp166, Lys168 is another important residue in the PKA active site. It is conserved in all Ser/Thr kinases and replaced by an Arg in the tyrosine kinases.[23,24] It interacts with the γ-phosphate in various crystals before and

(52) Ponder, J. W. *TINKER, Software Tools for Molecular Design*, version 3.6; The most updated version for the TINKER program can be obtained from J. W. Ponder's World Wide Web site at http://dasher.wustl.edu/tinker., February 1998.

(53) Mildvan, A. S. *Proteins* **1997**, *29*, 401−416.
(54) Kim, K.; Cole, P. A. *J. Am. Chem. Soc.* **1997**, *119*, 11096−11097.
(55) Kim, K.; Cole, P. A. *J. Am. Chem. Soc.* **1998**, *120*, 6851−6858.
(56) Williams, D. M.; Cole, P. A. *J. Am. Chem. Soc.* **2002**, *124*, 5956−5957.
(57) Parang, K.; Till, J. H.; Ablooglu, A. J.; Kohanski, R. A.; Hubbard, S. R.; Cole, P. A. *Nat. Struct. Biol.* **2001**, *8*, 37−41.
(58) Granot, J.; Mildvan, A. S.; Bramson, H. N.; Kaiser, E. T. *Biochemistry* **1980**, *19*, 3537−3543.
(59) Cook, A.; Lowe, E. D.; Chrysina, E. D.; Skamnaki, V. T.; Oikonomakos, N. G.; Johnson, L. N. *Biochemistry* **2002**, *41*, 7301−7311.
(60) Ablooglu, A. J.; Frankel, M.; Rusinova, E.; Ross, J. B. A.; Kohanski, R. A. *J. Biol. Chem.* **2001**, *276*, 46933−46940.

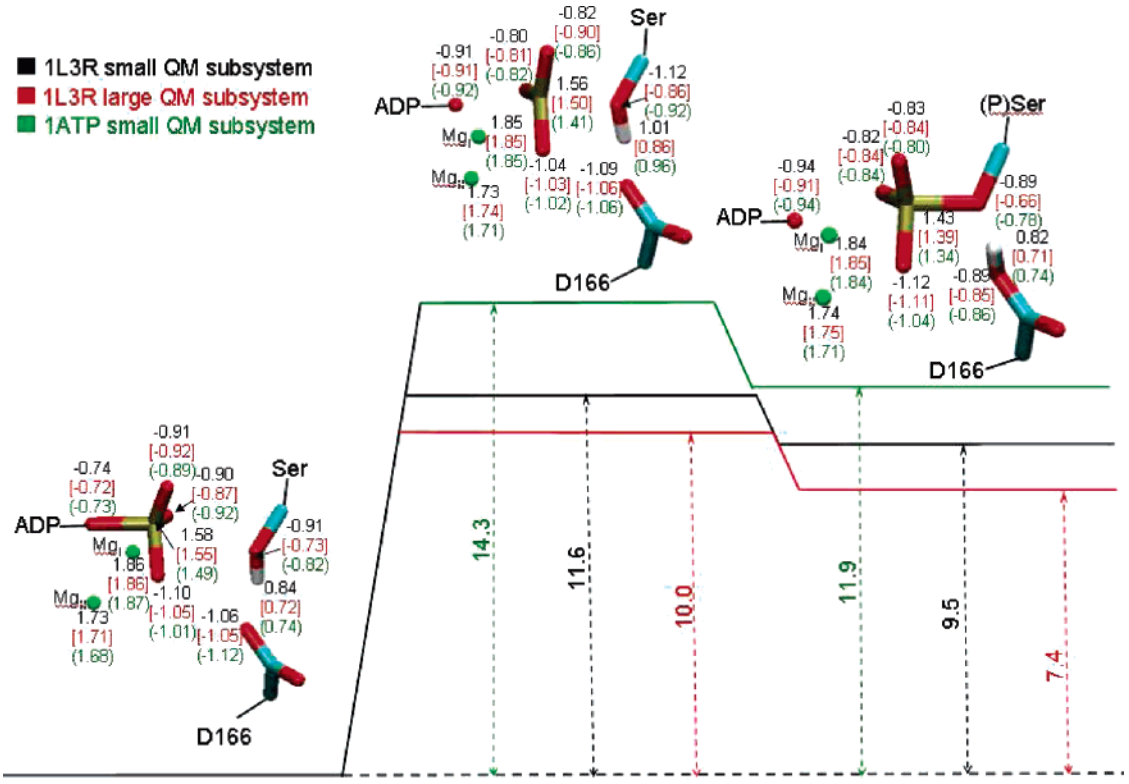

Figure 4. Calculated reaction scheme for the phosphoryl transfer step of 1L3R and 1ATP models. The values on the atoms indicate B3LYP/6-31+G* ESP charges for molecules in the QM subgroup (in au); the unit of the height of the barrier is kcal/mol.

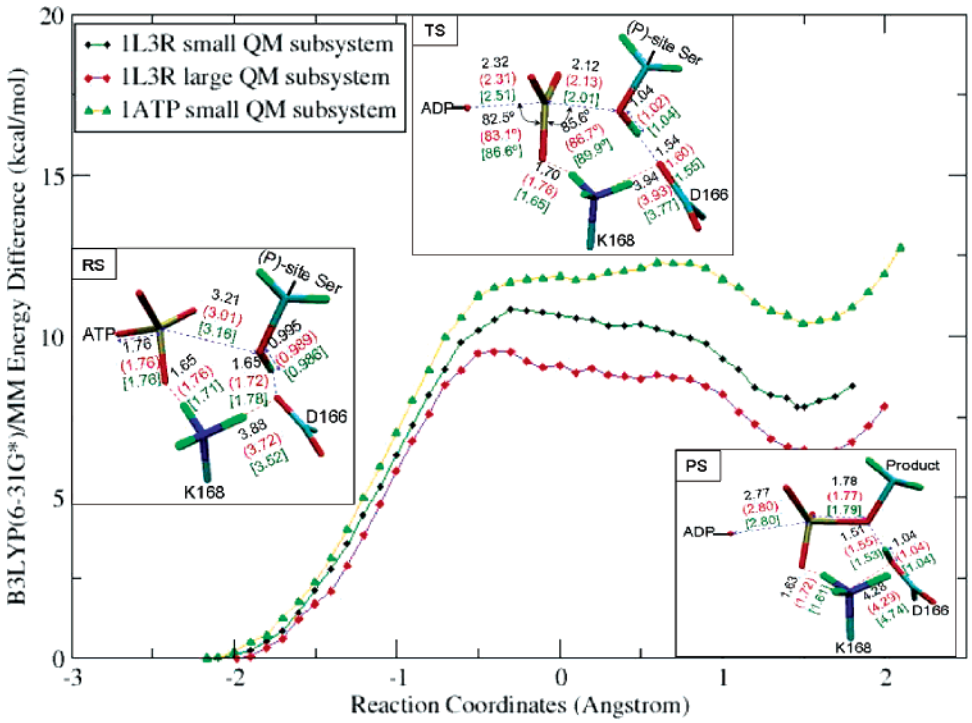

Figure 5. Determined minimum energy paths for the small and large QM/MM models of 1L3R. Distances between atoms involved in bond breaking and forming are given in angstroms.

after phosphoryl transfer,[19] and the replacement of Lys168 with Ala leads to large increases of K_m. There have been mainly two possible catalytic roles for this residue proposed in the literature: one is that it directly participates in the reaction by late transfer of one of its protons to the phosphate group, and the other is that it stabilizes the transition state through electrostatic interaction. We have conducted calculations to examine both hypotheses.

First we have conducted B3LYP(6-31G*) QM/MM calculations on the 1L3R small model to study whether the proton-transfer step between Lys168 and the phosphate group could take place. The results indicate that the transfer of a proton from

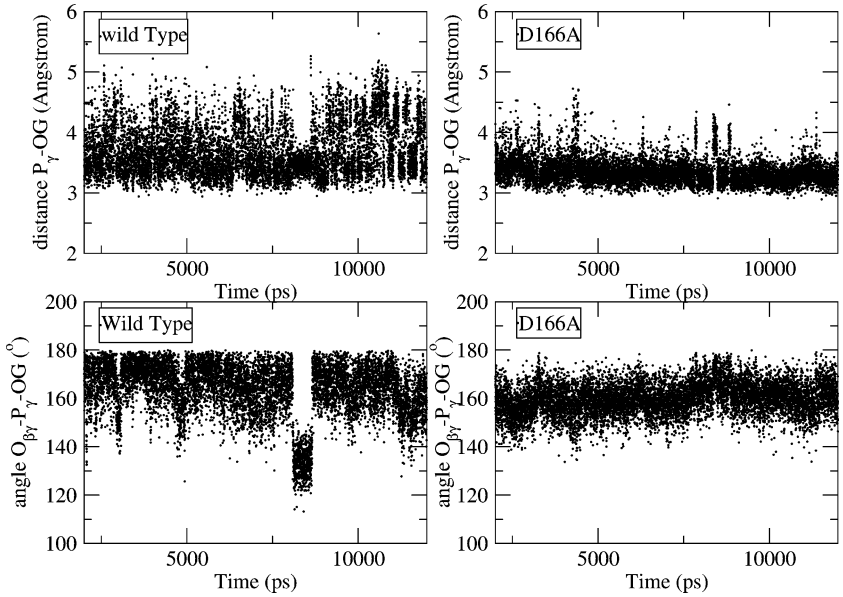

Figure 6. Distances between P_γ and the OG atom in the wild type and D166A mutation; the ATP−substrate alignment angle $O_{\beta\gamma}$−P_γ−OG in the wild type and D166A mutant.

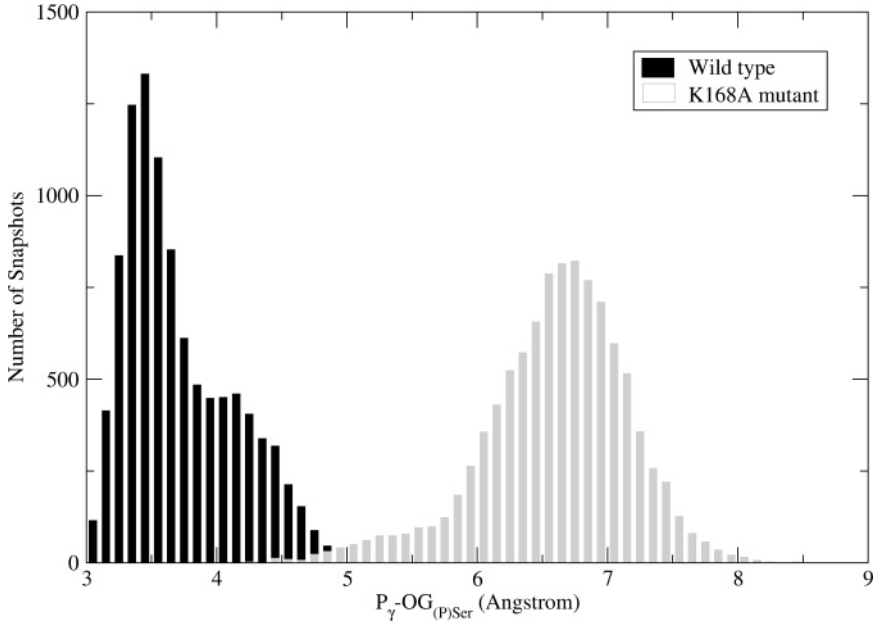

Figure 7. Time-dependent variation of separation of P_γ in ATP and the hydroxyl oxygen OG in P-site Ser. For the definition of OG and P_γ, cf. Figure 3.

Lys168 to the phosphate group is uphill, and the resulting product is destabilized by 3.3 kcal/mol. So our calculations do not support that Lys168 directly participates in the reaction. Then we conducted the calculations to test whether the role of Lys168 is to stabilize the transition state. Here one difficulty is that we have included Lys168 in the QM subsystem which makes it difficult to analyze its interaction with the rest of the active site. So we have conducted B3LYP(6-31G*) QM/MM calculations on the 1L3R model and 1ATP model with a even smaller QM/MM partition in which Lys168 is treated molecular mechanically, and we determined the reactant and transition states using the same procedure. We then analyzed the interaction between the Lys168 and the QM subsystem to determine its contribution to the stability of the transition state. Surprisingly, we found that the electrostatic interaction between Lys168 and the QM subsystem strongly destabilizes the transition state.

Our calculations so far do not support either of the hypotheses. So what is the catalytic role of Lys168? Here we mutated Lys168 with Ala in our 1L3R model and performed a 12 ns classical MD simulation on the K168A mutant with the same procedure as the wild type model. By analyzing the two trajectories and comparing their results, we found that although the K168A mutant has a very similar RMSD to that of the wild type, the distance between P_γ of ATP and the hydroxyl oxygen of the P-site Ser is significantly (on average 2.9 Å) longer in the K168A model than in the wild type, as shown in Figure 7. Moreover, The atomic mean-square fluctuations of Mg_2ATP in the K168A mutant is 0.18 Å^2 compared to 0.14 Å^2 in the wild type 1L3R. So our MD simulations indicate that the main catalytic role of Lys168 is to keep ATP and the substrate peptide in the near-attack reactive conformation. The larger distance between the ATP and the substrate peptide also indicates weaker

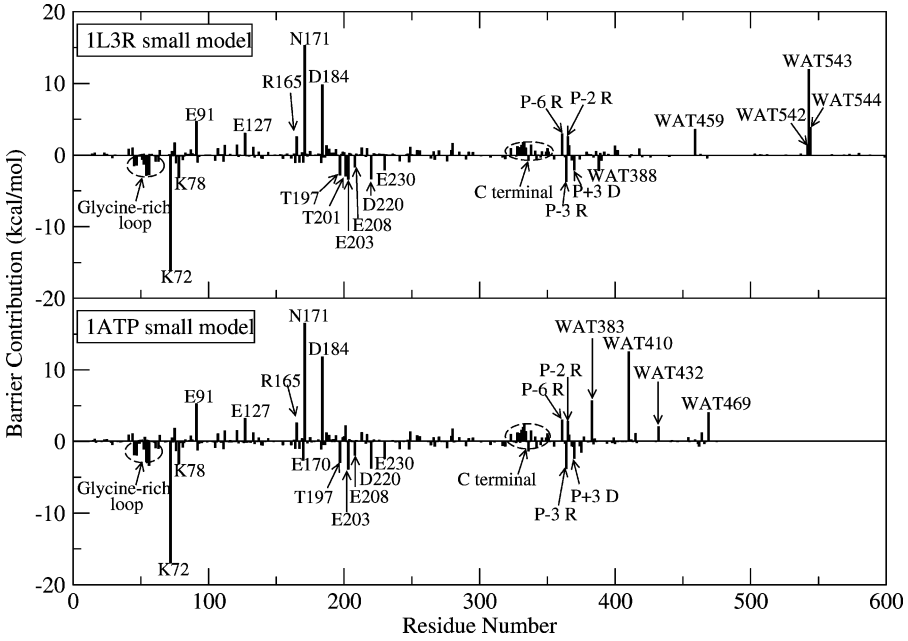

Figure 8. Individual MM residue electrostatic contribution to the transition state stabilization and destabilization.

binding of the peptide substrate, which is consistent with the mutagenesis result of increased K_m in yeast C-subunits.[5]

Catalytic Roles of Individual MM Residues Interacting with the Active Site. To understand the role of each residue in catalysis, we performed vdW and electrostatic energy contribution calculations between the QM subsystem and individual MM residues as the phosphorylation reaction proceeds from the reactant to the transition state based on the geometries of the small B3LYP(6-31G*) QM/MM models of 1L3R and 1ATP, respectively. While the results of the energy decomposition are suggestive, it must be recognized that the details would vary somewhat with the use of different models for the quantum mechanical or molecular mechanical calculations. Such analyses have been demonstrated to be able to provide detailed insights into enzyme catalysis,[40,41,43] among which some computational hypotheses[40,43] have been confirmed by later experimental studies.[43,61] The charges of the transition states (TS) and the reactant states (RS) were determined with B3LYP(6-31+G*)/MM calculation (MP2(6-31+G*)/MM calculation gives very similar results). The electrostatic and vdW interaction energies between the given residue and the QM subgroup were calculated classically for the reactant and transition state, respectively. The difference between the corresponding RS and TS results indicates the contribution of each residue to the reaction barrier. A negative number indicates that the residue stabilizes the TS, and vice versa. Since the effects of conformational change and dielectric screening are absent in our analysis and the original ab initio QM/MM calculations were performed variationally, we only use these numbers as a qualitative indicator, and not as a quantitative prediction. The vdW interaction change is generally quite small, therefore the results shown in Figure 8 only include the electrostatic interactions. We can see that the results for the two kinase structures are consistent with one another.

The glycine-rich loop is one of the most important motifs in the conserved protein kinase catalytic core. As discussed in the Introduction, it seems that there is some inconsistency between the suggestions from the structural studies[16] and the results from the mutation studies:[10,11] structural studies suggest that the loop may play an important role in stabilizing the transition state, while mutagenesis studies indicated that mutation of a single glycine has modest effects on the catalytic activity of PKA. Our calculation results for this structural unit are shown in Table 2. We can see that, despite the modest contributions of the individual residues in the loop to the barrier according to Figure 8, almost every residue in the whole loop (except Ser53) contributes to stabilize the transition state to some degree. The total contributions to stabilize the reaction barrier are 7.4 and 8.8 kcal/mol in 1L3R and 1ATP models, respectively. Thus, our calculation results indicate that the catalytic role of the glycine-rich loop comes from the collective effect rather than a single residue, and there is actually no inconsistency between the suggestions from the structural studies[16] and the results from the mutation studies.[10,11]

Table 2. Glycine-Rich Loop Individual Residue Contributions to the Transition State Stabilization or Destabilization for Two Crystal Structures (Calculation Based on B3LYP(6-31+G*)/MM Calculations)[a]

	$E_{ele+vdw}$	
residue	1L3R	1ATP
Lys47	−1.1	−2.0
Thr48	−0.1	−0.2
Leu49	−0.2	−0.3
Gly50	0.1	−0.1
Thr51	−0.8	−0.1
Gly52	−0.2	0.3
Ser53	0.6	1.1
Phe54	−2.2	−2.8
Gly55	−1.3	−1.3
Arg56	−2.2	−3.5
Val57	−0.0	−0.0
MM Total	−7.4	−8.8

[a] $E_{ele+vdw}$ refers to the total nonbonding interaction energy including electrostatic and vdW parts. "MM total" refers to the interaction between the total glycine-rich loop and QM subgroups. Energy units are in kcal/mol.

(61) Poyner, R. R.; Larsen, T. M.; Wong, S. W.; Reed, G. H. *Arch. Biochem. Biophys.* **2002**, *401*, 155−163.

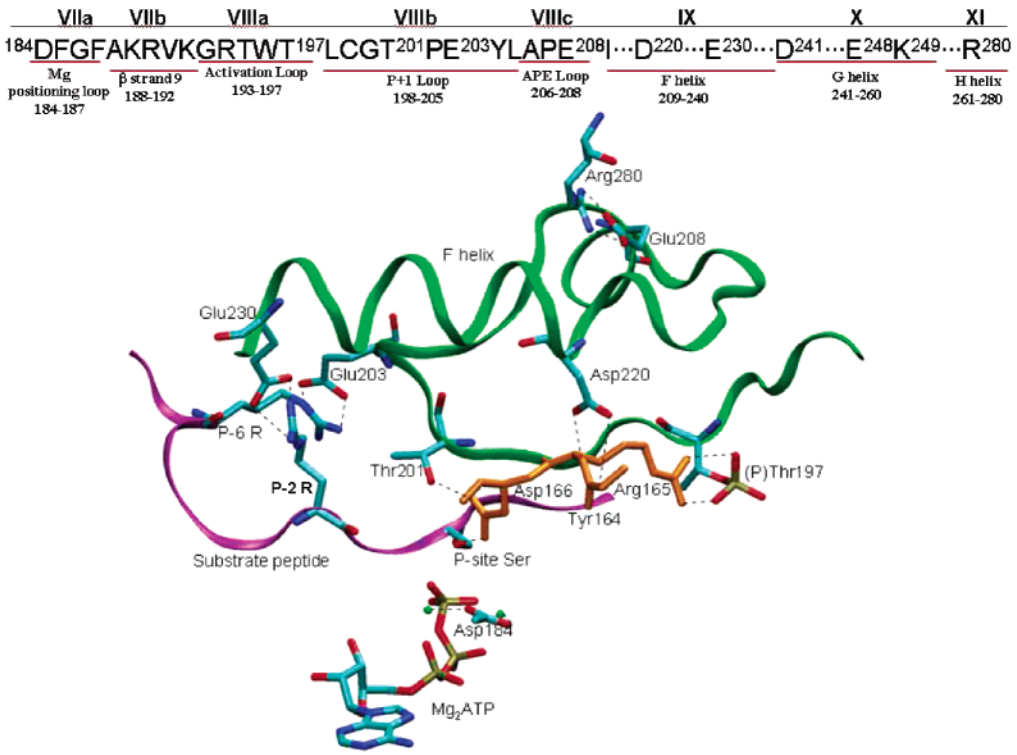

Figure 9. Individual nonbonding interactions between the residues 184−280 and the QM subgroup.

Residue Lys72 and Glu91 are another two conserved charged residues in the small lobe. Structural studies[19] have shown that Lys72 anchors α- and β-phosphate and Glu91 bridges to Lys72; cf. Figure 1b. The results in Figure 8 show that Lys72 strongly stabilizes the transition state through electrostatic interactions, while the Glu91 does not. Here we propose that the main role of Glu91 is to position the Lys72. Our finding that Lys72 strongly stabilizes the transition state is consistent with mutation studies[5] showing that replacement of Lys72 with Ala led to an 800-fold decrease in V_{max} with only a 5-fold increase in K_m(ATP).[5]

Lys78 is another transition-state stabilizer which contributes around 2∼2.5 kcal/mol. This residue lies in the C helix and has the potential to form hydrogen bonds with the carbonyl oxygens of Phe54 and Ser53 (d_{NZ-O} = 4.31 and 3.81 Å in 1L3R crystal) in the glycine-rich loop. The 12 ns MD simulation of the wild type 1L3R enzyme captured around 1% H-bonding between them. Glu127 lies in the ATP pocket, forming a hydrogen bond with the hydroxyl in the ribose of ATP. Our analysis indicates that it destabilizes the transition state. Experimental replacement with alanine decreases the reactivity of PKA to 2.3% of the wild type.[5] So we propose that the main role of Glu127 is likely to bind ATP in the right reactive conformation.

Although Arg165 destabilizes the transition state, it lies in the catalytic loop and forms two stable H-bonds with (P)Thr197. Experimental replacement of Arg165 with alanine decreases the reactivity of the kinase to 10.5% of the wild type.[5] Figure 9 shows that Arg165 has double hydrogen bonds with (P)Thr197 and directly links with Asp166, the catalytic base. The displacement of Arg165 essentially affects the hydrogen bonding network among ATP, P-site serine, and Asp166. Arg165 functions as the bridge to communicate between the activation loop and the active site. Asp220, anchoring the backbones of Arg165 and Tyr164 via hydrogen bonds, helps to hold the Arg165-Asp166 chain in the proper conformation and stabilizes the transition state.

Asn171 and Asp184 strongly destabilize the transition state and contribute over 10 kcal/mol to the transition state individually. Structurally, both of them bind to Mg^{2+} ions. We believe that these two residues are essential for binding Mg^{2+} ions, which provide stabilization to the transition-state (discussed later). The fact that replacement of Asp184 with Alanine made the PKA inviable emphasized such a role.[5] In addition, three active-site conserved waters, Asn171 and Asp184, all of which bond with the two conserved magnesium ions, extensively destabilize the transition state.

All the residues between Asp184 and Glu280 that interact with the QM subgroup by more than 0.8 kcal/mol have been listed in Table 3 and shown in Figure 9. (P)Thr197 contributes stabilization to the transition state, as do Glu203 and Glu230 by hydrogen bonding with the substrate peptide. Thr201 forms a hydrogen bond with Asp166 and contributes to stabilize the transition state in the 1L3R model but somehow destabilizes in the 1ATP model. The role of this conserved residue is still not clear. Experimental replacement with Ala impaired the ability to autophosphorylate Thr197 and abolished activity because of steric factors.[62,63] In our calculation models, Lys168 bridged the phosphate to the peptide via an −OH of Thr201. To sum up, the overall catalytic effect for the residues between Asp184 and Glu280 is to stabilize the transition state more than 12 kcal/mol. Another conserved water, WAT459 in 1L3R (WAT383 in 1ATP), forming a bridge between the OD1 of Asp166 and the carbonyl oxygen of Leu167, destabilizes the transition state by 3.6 kcal/mol in 1L3R and 5.7

(62) Moore, M. J.; Kanter, J. R.; Jones, K. C.; Taylor, S. S. *J. Biol. Chem.* **2002**, *277*, 47878−47884.
(63) Moore, M. J.; Adams, J. A.; Taylor, S. S. *J. Biol. Chem.* **2003**, *278*, 10613−10618.

Table 3. Individual Residue Contributions to the Transition State Stabilization or Destabilization ($|\Delta E_i^{tot}| \geq 0.8$ kcal/mol) (Calculation Based on B3LYP(6-31+G*)/MM Calculations)[a]

categories[b]	residue	$\Delta E_{i,1L3R}^{vdw+ele}$	$\Delta E_{i,1ATP}^{vdw+ele}$	region[c]
		from RS to TS		
1	Lys213	0.8	1.3	IX
	Lys249	1.1	1.6	X
	Arg280	1.2	1.8	XI
2	(P)Thr197	−1.8	−2.6	VIIIa
	Glu203	−3.4	−4.7	VIIIb
	Glu208	−1.2	−1.9	VIIIc
	Asp220	−1.9	−3.3	IX
	Glu230	−1.9	−2.8	IX
	Glu241	−1.0	−1.4	X
	Glu248	−0.9	−1.3	X
3	Thr201	−4.2	0.6	VII
MM total		−13.4	−12.6	

[a] vdW refers to the van der Waals interaction energy, and ele refers to the electrostatic interaction energy. "MM Total" refers to the interaction of all residues between Asp184 and Arg280 and QM subgroups. Energy units are in kcal/mol. [b] The residues in the first category are the positively charged and destabilize the transition state. The residues in the second category are those having negative charges and stabilizing the transition state. The third category includes the residues which have no net charges. [c] The regions correspond the different subdomains, as defined by Hanks et al.[66]

Table 4. Interaction between Individual Mg^{2+} Ions with the Rest of the Atoms in the QM Subgroup (the Energy Unit Is kcal/mol)

	B3LYP(6-31+G*)/MM		MP2(6-31+G*)/MM	
	1L3R	1ATP	1L3R	1ATP
		Mg_I		
Δ(TS−RS)	−12.4	−30.9	−13.4	−33.4
Δ(Int-RS)	−42.9	−40.9	−46.6	−43.9
		Mg_{II}		
Δ(TS−RS)	−40.1	−83.8	−45.0	−92.6
Δ(Int-RS)	−86.0	−91.6	−96.0	−100.7

kcal/mol in 1ATP. So the role of this water is apparently structural.

Several charged residues in the substrate peptide affect the stabilization of the transition-state, too. P-6 and P-2 Arg destabilize the transition state, while P-3 Arg and P+3 Asp always stabilize the transition state. To sum up, the net effect is that the transition state is stabilized slightly, i.e. −0.6 kcal/mol in 1L3R and −1.1 kcal/mol in 1ATP.

Role of the Two Mg^{2+} Ions. In PKA studies, Mg_I (binding with β- and γ-phosphates) is generally identified as a catalytic activator, while Mg_{II} (binding with α- and γ-phosphates) as an inhibitor. A more thermostable conformation, secured by two metal sites being occupied, appears to switch with a catalytically more active but less thermostable conformation with one metal site occupied.[64,65] In our calculations, although the two magnesium ions are treated quantum mechanically, the charges on the magnesium ions change very little from the reactant to the transition state and to the product. So we have calculated the classical electrostatic interaction energies between the magnesium ion and the rest of the QM subsystem without magnesium ions, as shown in Table 4. We can see that both metal ions contribute greatly to lower the transition state barrier through electrostatic interactions. Mg_{II} contributes even more stabilization to TS than Mg_I, which seems to be inconsistent with the experimental results.[64,65] Here we make the following two hypotheses. First, the role of the two magnesium ions is to activate the phosphoryl transfer, while residues such as Asn171 and Asp184 and several active-site conserved waters binding with them destabilize TS and play an "inhibitory" role. When only one magnesium ion is bound, those anchoring residues will also be positioned differently and may have less inhibitory effect on the reaction. The second reason is that the rate determining step is the dissociation of the product, so that the enzyme with one magnesium ion bound, which is less thermostable, may have larger conformational fluctuations to facilitate the product release.

4. Conclusions

The phosphoryl transfer reaction catalyzed by the catalytic subunit of cAMP-Dependent Protein Kinase has been studied by density functional theory QM/MM calculations. Using different initial structures, the calculated reaction barrier at the B3LYP QM/MM level is 11.6 kcal/mol for an initial structure coming from a crystal mimic of the transition state, while it is 14.3 kcal/mol for an initial structure coming from a reactant complex mimic, which are very consistent with the experimental estimation of 13.8 kcal/mol.

Our calculations confirm that the phosphorylation reaction proceeds through a symmetric transition state, and then Asp166 serves as the catalytic base to accept the proton delivered by the substrate peptide. Although Lys168 strongly destabilizes the transition state in the phosphoryl-transfer step and does not directly participate in the reaction, our 12 ns molecular dynamics simulations on both wild type and K168A mutant, respectively, demonstrate that the catalytic role of Lys168 is to keep ATP and substrate peptide in the near-attack reactive conformation.

Barrier decomposition analysis qualitatively explained individual residue contributions in the whole enzyme. The glycine-rich loop, providing both hydrophobic and electrostatic interactions with ATP or ADP, always stabilizes the transition state. Lys72, binding with nontransferable phosphates of ATP, strongly stabilizes the transition state, while Lys168, Arg171, and Asp184 strongly destabilize the transition state. Although most of the residues in the large domain are not located in the active site, the overall effect is to stabilize the transition state. The role of Mg^{2+} ions appears to stabilize the transition state through electrostatic interactions, although the residues as well as water molecules binding to Mg^{2+} ions mainly play a structural role and destabilize the transition state.

Acknowledgment. This work has been supported in part by grants from the NSF and NIH. Additional support has been provided by NBCR, CTBP, HHMI, the W. M. Keck Foundation, and Accelrys, Inc.

JA0464084

(64) Adams, J. A.; Taylor, S. S. *Biochemistry* **1992**, *31*, 8516−8522.
(65) Herberg, F. W.; Doyle, M. L.; Cox, S.; Taylor, S. S. *Biochemistry* **1999**, *38*, 6352−6360.
(66) Hanks, S. K.; Hunter, T. *FASEB J.* **1995**, *9*, 576−596.